THE JOURNAL OF PHYSICAL CHEMISTRY C

Article

pubs.acs.org/JPCC

Gate-Induced Intramolecular Charge Transfer in a Tunnel Junction: A Nonequilibrium Analysis

Adva Baratz,[†] Michael Galperin,*[,‡] and Roi Baer*[,†]

[†]Fritz Haber Center for Molecular Dynamics, Institute of Chemistry, the Hebrew University of Jerusalem, Jerusalem 91904, Israel

[‡]Department of Chemistry and Biochemistry, University of California at San Diego, La Jolla, California 92093, United States

ABSTRACT: A recently introduced molecular junction, for which the gate acts as an on/off switch for intrajunction electron transfer between localized donor and acceptor sites is studied. We demonstrate that a Landauer + density functional (DFT) approach is fundamentally flawed for describing the electronic conductance in this system. By comparing the Landauer + DFT conductance to that predicted by the Redfield quantum master equations, we point out several effects that cannot be explained by the former approach. The molecular junction is unique in the small number of conductance channels and their sharp response to the gate.

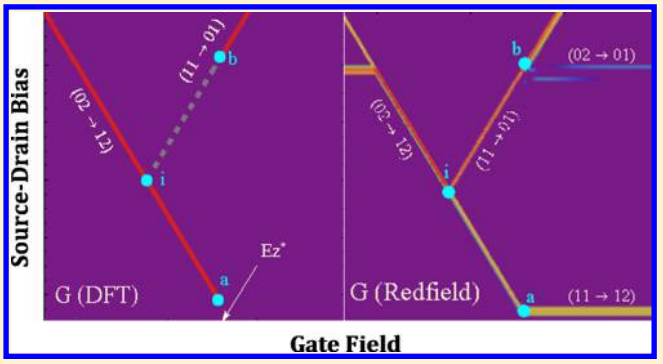

I. INTRODUCTION

In a recent paper,[1] two of us presented a molecular junction in which confinement and Coulomb effects are pronounced and controlled by well-understood physical principles. A schematic depiction of the system is given in Figure 1, describing a benzene-malononitrile (MN) acceptor displaced by a vertical distance $\bar{z}$ with respect to the *trans*-polyacetylene (PA) donor.

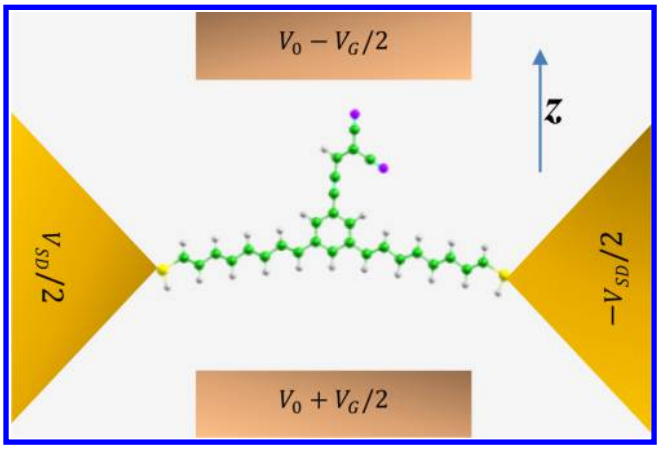

Figure 1. Schematic depiction of the molecular junction in ref 1: two thiol-terminated *trans*-polyacetylene (PA) segments ($SH-(HC=CH-)_4$) acting as meta substituents on the aromatic ring of a benzene-malononitrile (MN) molecule. The gate potential V_0, the gate bias V_G, and the source drain bias V_{SD} are adjustable. The PAs are electron donors determining the ionization potential of the molecule ($I \sim 6.2$ eV). The MN is an electron acceptor, endowing the molecule with electron affinity $A \sim 1.2$ eV. DFT calculations showed that a gate field beyond a critical value of $E_z^* = 0.63$ V/Å inspires spontaneous electron transfer from donor (PA) to acceptor (MN).

The energy gap E_g for intramolecular electron transfer thus becomes dependent on the gate field E_z: $E_g(E_z) = I - A - e\bar{z}E_z$, where e is the electron charge and I and A are the ionization and affinity energies, respectively (see caption of Figure 1). A sufficiently strong gate field, beyond a critical value E_z^*, will induce electron transfer from donor to acceptor, allowing sensitive control over the electronic properties of the junction.

Our previous analysis of this junction[1] was carried out using a generalized Kohn−Sham (GKS) density functional theory (DFT) where the molecular electronic wave function is mapped onto a wave function of noninteracting electrons having identical single electron density. It is common to use the conductance of the noninteracting system as an approximation for the conductance of the interacting system[2−5] using the Landauer equation[6] which assumes that the population of states on the molecule does not affect its transmission probability. There are two problems usually associated with such an approach. One has to do with the missing derivative discontinuities and self-interaction energies appearing in most applications of DFT that use local or hybrid approximations causing the orbital energies to deviate significantly from the ionization potentials, the so-called quasiparticle energies.[7,8] We deal with this problem by using a range-separated hybrid where a first-principles tuning of the range parameter mitigates the missing derivative discontinuities and aligns the orbital and quasiparticle energies.[9−11] The second problem has to do with how to reconcile the fact that the Landauer theory assumes that electron transmission is insensitive to the population with the fact that for interacting electrons they have a strong effect (for example, in the Coulomb blockade regime). Here we rely on

Received: December 27, 2012
Revised: April 20, 2013
Published: April 22, 2013

the KS/GKS Hamiltonian to take the nonequilibrium population effects into account, while the conductance itself is still "noninteracting". Such methodology is a common approach with Coulomb blockade problems which has been described using unrestricted spin DFT.[12]

In our previous work, we found additional issues which as we now show cannot be solved, even approximately within the DFT + Landauer approach. The Landauer differential conductance channels of the junction closely follow the location of two orbital energies $\varepsilon_\uparrow$ and $\varepsilon_\downarrow$ corresponding to the orbital ψ_A on the acceptor site of the molecule. These orbital energies change continuously as the gate field E_z increases. However, a discontinuity occurs passing through the *critical* gate field E_z^* where $\varepsilon_\uparrow$ drops in energy below the HOMO energy ε_H of the molecule (thus ψ_A gets filled by a spin-↑ electron), and the orbital energy $\varepsilon_\downarrow$ increases in energy due to onsite Coulomb repulsion (see schematic orbital energies in the left part of Figure 2). Thus, there are two

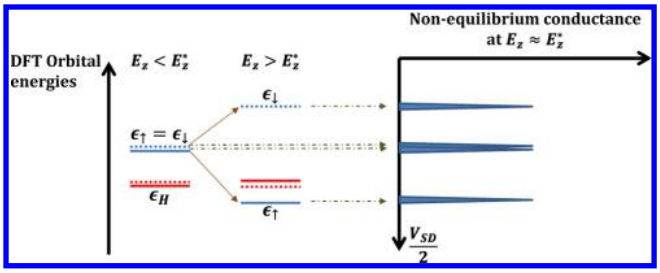

Figure 2. Left: Schematic depiction of the DFT orbital energies for two gate fields: (1) $E_z < E_z^*$ where the orbital energies are degenerate in energy ($\varepsilon_\uparrow = \varepsilon_\downarrow$) and (2) $E_z > E_z^*$ where the orbital energies become spin dependent and split $\varepsilon_\uparrow < \varepsilon_\downarrow$. Right: schematic depiction of the conductivity as a function of source-drain bias for $E_z \approx E_z^*$ where the four channels can coexist in the nonequilibrium conducting mix state but no single particle Hamiltonian can describe two spin polarized conduction channels using just a one spin polarized orbital.

qualitatively different GKS Hamiltonians, one corresponding to the small gate field, $E_z < E_z^*$, and the other corresponding to the high gate field, $E_z > E_z^*$. Because the placement of orbital energies corresponds to quasi-particle energies, as long as E_z is very different from E_z^* and bias is not too large, it may be argued that one of these two GKS-DFT Hamiltonians can serve as a basis for computing the conductance using Landauer's theory. Each GKS Hamiltonian represents a different non-equilibrium population with respect to the applied gate field. If, however, we wish to study the conductance of the junction at gate fields *close* to the critical gate E_z^* both conductance patterns stemming from the two Hamiltonians are expected to appear simultaneously, and four conductance peaks will necessarily show up in the right part of Figure 2: two peaks corresponding to the nonequilibrium electronic state at $E_z < E_z^*$ and two corresponding to that at $E_z > E_z^*$. Clearly, there is no single KS/GKS Hamiltonian that can describe such a conductance pattern because the energy levels of such a single-electron Hamiltonian have only two orbital energies associated with ψ_A and will therefore always miss two out of the four conductance channels appearing in Figure 2.

In view of this limitation, this paper departs from DFT and analyzes the conductance of the molecule using a double quantum dot model, with parameters based on the GKS-DFT results. The model is described in section II. We first analyze (section III) the dependence of the eigenenergies on the gate potential assuming no external bias is involved. We explain why a KS/GKS approach will reproduce only this picture, which does not take into account the full nonequilibrium population of molecular states. Next we discuss the full nonequilibrium treatment (section IV). There are several ways for calculating the conductance in the Hubbard model where a non-equilibrium distribution of molecular states is present, for example, real-time perturbation theory,[13−16] generalized quantum master equation schemes,[17−21] nonequilibrium quasiparticles,[22−28] and Hubbard Green functions.[29−33] We base our treatment on one of the simplest approaches, appropriate for weak molecule−lead coupling, namely, the Redfield and Lindblad quantum master equation formulations.[34−39] We discuss the resulting conductance patterns in view of the simpler but wrong KS/GKS picture. The results are summarized in section V.

II. HUBBARD MODEL OF THE JUNCTION

Our model assumes that only frontier orbitals are active in the junction. From the DFT calculation, we find that the HOMO and HOMO-1 orbitals, located on the left and right PA strands, respectively, are almost degenerate. We further found that these orbitals do not contribute to the conductance (because of an interference effect associated with the benzene ring[1]), and their primary effect is to act as electron donors. For this reason, we consider only one of these orbitals in our model (QD2 in Figure 3) and do not couple it directly to the leads.

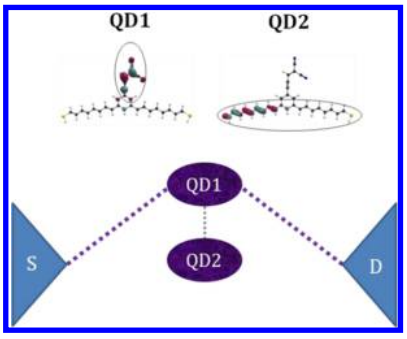

Figure 3. Schematic diagram of the double quantum-dot model. QD1 represents the LUMO (localized on the MN acceptor) and QD2 the HOMO (localized on the PA donor) of the molecule. The two quantum dots couple to each other, but only QD1 is directly coupled to the source and drain because of a destructive interference effect.

From the DFT calculation we find that the LUMO orbital has a dual role: it acts both as an electron acceptor from the donor and as a direct channel for conductance. We thus model it as a quantum dot (QD1) which is coupled to the leads with coupling parameter Γ. These two QDs form our model for the junction, which we describe now in detail with model parameters summarized in Table 1. The 2QD Hubbard Hamiltonian for the junction is

$$\hat{H}_{\mathrm{Hub}} = \sum_{i=1}^{2} \varepsilon_i(E_z)\hat{n}_i + t \sum_{\sigma=\uparrow\downarrow} (\hat{a}_{1\sigma}^{\dagger}\hat{a}_{2\sigma} + HC) + \sum_{i=1}^{2} U_i \hat{n}_{i\uparrow}\hat{n}_{i\downarrow} \quad (1)$$

where $\hat{a}_{i\sigma}^{\dagger}$ ($\hat{a}_{i\sigma}$) are the electron creation (annihilation) operators for QD I spin σ (i = 1,2 and ↑,↓). $\hat{n}_{i\sigma} = \hat{a}_{i\sigma}^{\dagger}\hat{a}_{i\sigma}$ is the spin-dependent occupation of QD i, and $\hat{n}_i = \hat{n}_{i\uparrow} + \hat{n}_{i\downarrow}$ is the number of electrons on the QD. The first term in $\hat{H}_{\mathrm{Hub}}$ describes the single particle site energies, where ε_i is the orbital

dx.doi.org/10.1021/jp312776c | J. Phys. Chem. C 2013, 117, 10257−10263

Table 1. Energetic Parameters of the Many-Body Model, Equation 4

parameter	value (eV)	explanation
μ	−5.1	Fermi level of gold
$\varepsilon^{\mathrm{HOMO}}$	−6.2	from DFT calculation
$\varepsilon^{\mathrm{LUMO}}$	−1.2	from DFT calculation
ε_2^0	−7.8	$\varepsilon^{\mathrm{HOMO}}$ of PA^+ (from DFT)
ε_1^0	−1.2	$\varepsilon^{\mathrm{LUMO}}$
U_1	4.5	$\alpha - \beta$ splitting in DFT
U_2	1.6	$U_2 = \varepsilon^{\mathrm{HOMO}} - \varepsilon_1^0$
U_{12}	1.8	DFT exciton binding energy
$\Gamma_{1L} = \Gamma_{1R}$	0.0005	see text for explanation
t	0.001	see text for explanation
q_1	0	see text for explanation
q_2	2	see text for explanation
k_BT	0.001	

energy of an electron in QD i where the orbital energies are gate-field dependent

$$\varepsilon_i(E_z) = \varepsilon_i^0 - ez_iE_z \tag{2}$$

where E_z is the gate field in direction z and z_i is the vertical position of QDi. ε_1^0 is taken as the LUMO energy of the molecule. Since QD2 holds in the molecular ground state two electrons, ε_2^0 is the energy to put the first electron on QD2; i.e., it is the HOMO energies of the molecular *cation*. Due to the vertical displacement of the acceptor relative to the donor, the gate field controls the orbital energy difference $\varepsilon_1 - \varepsilon_2$. It is possible to fix the energy of ε_2 so that only ε_1 is gate-field dependent (in the model we do this by taking $z_2 = 0$ in eq 2). As for the dipole moment, ez_1, we take its value from ref 1 as 5.1 eÅ. Achieving this in a laboratory setup (as in Figure 1) requires careful tuning of the metallic potentials.[40]

The second term in $\hat{H}_{\mathrm{hub}}$ couples QD1 to QD2 using the hopping parameter t which enables the charge transfer between QD1 and QD2. The small overlap between HOMO and LUMO in this system dictates a small value of t, and we employ $t = 0.001$ eV as a representative value of such weak coupling. Note that this weak coupling does not have a significant effect on the physical results discussed in the paper.

The third term in $\hat{H}_{\mathrm{hub}}$ is the on-site Hubbard repulsion determined by the parameters U_i. The value of U_1 is equal to the difference between the spin-up and spin-down LUMO energies in the GKS/BNL* calculations (see ref 1). The value of U_2 fulfills the equation

$$\varepsilon^{\mathrm{HOMO}} = \varepsilon_2^0 + U_2 \tag{3}$$

where $\varepsilon^{\mathrm{HOMO}}$ and ε_2^0 are the DFT/BNL* HOMO energy of the neutral and cation molecule, respectively.

In ref 1 we found that the long-range interaction between the electron on QD1 and the hole on QD2 formed by intramolecular charge transfer is an important energy scale. To consider this effect, we add to the Hubbard Hamiltonian intersite Coulomb interaction terms, forming the molecular junction Hamiltonian

$$\hat{H}_{\mathrm{M}} = \hat{H}_{\mathrm{Hub}}(E_z) + U_{12}(q_1 - \hat{n}_1)(q_2 - \hat{n}_2) - \mu\hat{N} \tag{4}$$

where for convenience of discussion we include in $\hat{H}_{\mathrm{M}}$ the chemical potential of the leads μ, and $\hat{N} = \Sigma_{i=1}^{2}\hat{n}_i$ is the number of electrons on the molecule. The parameters q_i are the positive charges on each quantum dot. Under zero bias and gate, the donor site QD2 is electrically neutral, and since it represents the molecular HOMO it holds two active electrons and thus also has a static ("nuclear") charge of $q_2 = 2$. The acceptor site QD1 is also electrically neutral at zero bias, and since it represents the molecular LUMO it holds no active electrons and thus has a static charge of $q_1 = 0$.

The left/right leads are modeled by noninteracting electron Hamiltonians $H_{\mathrm{L/R}} = \Sigma_{k,\sigma}\varepsilon_k\hat{c}^{\dagger}_{\mathrm{L/R},k\sigma}\hat{c}_{\mathrm{L/R},k\sigma}$, where $\hat{c}^{\dagger}_{\mathrm{L/R},k\sigma}$ ($\hat{c}_{\mathrm{L/R},k\sigma}$) are the creation (annihilation) operators and ε_k the orbital energies or quasiparticle energies in the leads. QD1 is coupled to the leads via the term $\Sigma_{k,\sigma}(V_k a^{+}_{1\sigma}c_{\mathrm{L/R},k\sigma} + HC)$ with V_k being the coupling parameters. We are interested in this work in the weak molecule−electrode coupling limit, thus the escape rate $\Gamma_{\mathrm{L/R}}(\varepsilon) = 2\pi\Sigma_k|V_k|^2\delta(\varepsilon - \varepsilon_k)$ is assumed energy independent and taken as $\Gamma_{\mathrm{L/R}} = 0.0005$ eV, which is considerably smaller than the value of the hopping parameter t and the temperature.

We now discuss the energy levels of the Hamiltonian of eq 4 assuming $t \to 0$, henceforth called the "diabatic" limit. The state occupations n_1 and n_2 are good quantum numbers, and the energies can be labeled as (n_1n_2). Some are shown in the top panel of Figure 4 as a function of the gate field E_z. At low gate fields the ground state is (02), but as E_z grows, the charge-transfer state (11) descends in energy (due to the dependence of ε_1 on E_z, see eq 2) and crosses (02) to become the ground state of the system once $E_z > E_z^*$, where $E_z^* = 0.63$ V/Å is the critical gate field mentioned in the Introduction. Two other low-lying states are plotted: one is the positively charged (01) state, with energy not dependent on E_z (since $n_1 = 0$), and the second is the negatively charged state (12) with energy descending with E_z.

III. CONDUCTANCE ASSUMING EQUILIBRIUM POPULATION OF MOLECULAR STATES

In equilibrium at low temperature, the junction is in its ground state, and conductance channels are formed by a transition to low-lying states which differ from the ground state by an electron or by a hole. Assuming a symmetric potential drop across the junction, the source−drain potential difference V_{SD} required for a transition $(n_1n_2) \to (n_3n_4)$ is

$$V_{\mathrm{SD}} = 2\Delta E(n_1n_2 \to n_3n_4)/e \tag{5}$$

In Figure 4 (bottom), we plot the "transition channels" obeying this relation as a function of the gate field E_z. At $E_z < E_z^*$, the blue shaded region, the ground state is (02), and the possible transitions are to states (12) requiring energy $2\Delta E(02 \to 12)$ and to (01) requiring energy $2\Delta E(02 \to 01)$ (see red and black solid lines in the blue shaded region of Figure 4 (bottom)). For $E_z > E_z^*$, the pink shaded region, the ground state becomes (11), and the possible transitions are to state (01) requiring energy $2\Delta E(11 \to 01)$ or to state (12) requiring $2\Delta E(11 \to 12)$ (see red and black solid lines in the pink shaded region of Figure 4 (bottom)). The two remaining transition channels, $(11 \to 21)$ and $(11 \to 10)$, are not considered since they appear at much higher energies.

In the diabatic limit ($t \to 0$), the transport of charge through QD2 is not possible since this dot is decoupled from the leads. Therefore, of the four channels described above, only two, those involving a change in n_1, actually conduct. These two channels are colored red in Figure 4 (bottom). When $E_z < E_z^*$, the electron conductance channel $(02 \to 12)$ is operative as (02) is the ground state. Similarly, when $E_z > E_z^*$ only $(11 \to 01)$ is active as (11) is the ground state. These considerations

dx.doi.org/10.1021/jp312776c | J. Phys. Chem. C 2013, 117, 10257−10263

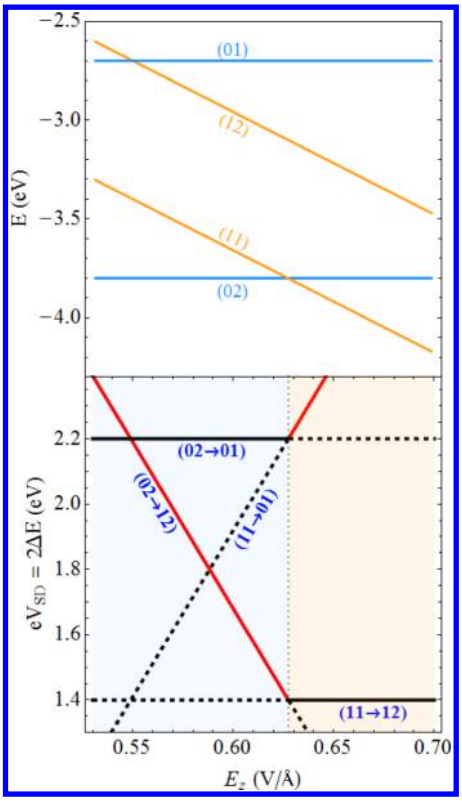

Figure 4. Top panel: Low-lying "diabatic" ($t \to 0$) eigenenergies of the model Hamiltonian in eq 4 as a function of gate field E_z. The states are designated as $(n_1 n_2)$. Bottom panel: Selected diabatic energy *differences* (multiplied by 2) from the ground state to the nearest hole/electron states as a function of E_z. These can be considered as transition channels in the V_{SD}–E_z plane. The blue (pink) shaded area designates $E_z < E_z^*$ ($E_z > E_z^*$) where (02) ((11)) is the ground state and $E_z^* = 0.63$ V/Å is the critical gate field. It is at this gate field that the conductance described by the DFT–Landauer approach ought to break down. The red lines are transition channels that should be active according to the DFT–Landauer assumption of a single ground-state distribution. The black dotted portion of each line is the regime where this transition channel should not be active due to lack of population of the relevant state. The solid black lines are transition channels that should not be active in the diabatic limit ($t \to 0$) since in this limit QD2 is decoupled from the leads (see text below for details).

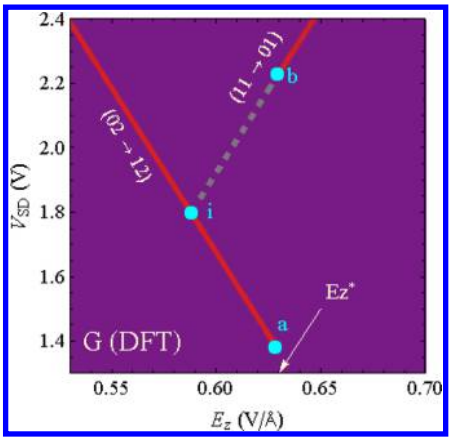

Figure 5. Expected position of the differential conductance peaks as a function of gate field E_z and source-drain bias V_{SD} at $t \to 0$ based on a KS/GKS DFT–Landauer theory. In such a case the KS/GKS Hamiltonian is that of the (02) ground state when $E_z < E_z^*$ and that of the (11) ground state when $E_z > E_z^*$. Accordingly, there are two conducting channels,[41] which can be assigned to the transitions (02 → 12) and (11 → 01). At gate fields below E_z^* the active channel (02 → 12) is electron conducting, while for $E_z > E_z^*$ the active channel (11 → 01) is hole conducting. The intersection of the red line (02 → 12) with the extrapolated (dotted) line (11 → 01) is marked by the point i, while points a and b denote, respectively, the ending and the beginning of those channels which occur at the critical gate field E_z^*. When the gate and bias are set to point i we find a breakdown of the DFT–Landauer description: there is only one LUMO, and it cannot account for both conductance channels ia and ib simultaneously.

allow us to deduce the position of the expected differential conductance peaks as a function of gate field E_z and source–drain bias V_{SD} shown in Figure 5. It is not surprising that this conductance map is similar to that reported in ref 1 which was obtained by using the KS/GKS DFT–Landauer approach. The KS/GKS DFT Hamiltonian is also essentially a "hostage" of the ground state; as we explained above it cannot account for the second low-lying state because of a lack of orbitals. Therefore, for each gate field it can only have one active channel corresponding to the ground state of the molecule. The "missing" orbital is seen in Figure 5 as a dotted line.

IV. EFFECT OF NONEQUILIBRIUM POPULATION OF MOLECULAR STATES

The considerations above relied on a simplifying assumption, namely, that the bias does not modify the population distribution of molecular states, and so at each gate field only the ground state of the molecule is populated. We now lift this assumption since we use quite large bias voltages and turn to a more realistic treatment of the junction that allows non-equilibrium population distribution on the molecule. We employ the Redfield QME, where the weak coupling to the leads is treated as a perturbation. A standard closure procedure allows us to obtain an effective Liouvillian in the molecular subspace. The right eigenvector corresponding to an eigenvalue with zero imaginary part is the steady-state density matrix (SSDM). From the SSDM we compute the steady-state populations, current $I(V_{SD})$, and the differential conductance $G = \partial I/\partial V_{SD}$ as a function of V_{SD} for each gate field.

One well-known shortcoming of Redfield theory is that its SSDM is not guaranteed to be positive definite, as a physical density matrix (DM) should always be. Indeed, in our calculations we do find certain voltage regimes where Redfield QME fails. However, these are not the regimes of interest for this work. Note that we have also used the Lindblad approach[34,35] to compute the conductance and populations and obtained nearly identical results to those of the Redfield theory in the regimes of interest shown below. The Lindblad approach guarantees positivity of the DM, although it has other basic shortcomings.[36] It is comforting that in the regime of interest both methods gave identical predictions.

We now discuss the results we obtained for the molecular state populations P, the steady-state currents I, and the differential conductance peaks G as functions of E_z and V_{SD} (see Figure 6).

A. Population Distribution of Molecular States. The population distribution among the four low-lying molecular states, depicted in the left panel of Figure 6, displays a variety of domains. To facilitate the interpretation we used a different color for each domain with border lines dictated by the transition channels and appear in black. Each domain is characterized with a different combination of states. The most populated state appears in large bold letters at the center of

dx.doi.org/10.1021/jp312776c | J. Phys. Chem. C 2013, 117, 10257–10263

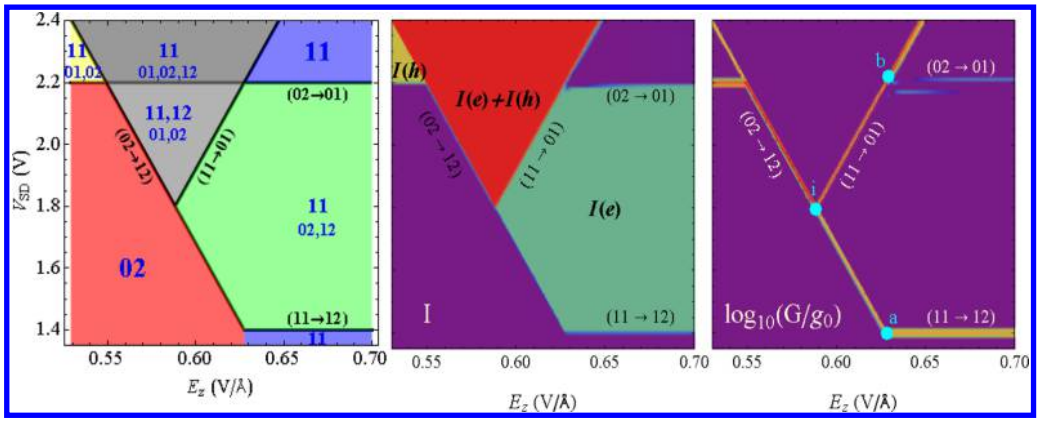

Figure 6. Contour plots of the Redfield prediction for the steady-state distribution of populations $P(02)$, $P(11)$, $P(12)$, and $P(01)$ (left panel), current I (middle panel), and the differential conductance peaks G (right panel) as functions of E_z and V_{SD}. The colors of the different population distribution regimes (left panel) are chosen arbitrarily. The border lines for those regimes are the transition channels discussed in section III, and for each regime, the most populated state is denoted by bold letters. The color coding for the current and differential conductance peaks (middle and right panels) has a meaning of intensity (red, orange, yellow, green, blue, and purple, where red is the highest and purple is zero). The maximum current (in atomic units) is $I \approx 1 \times 10^{-5}$, and the maximum conductance is $G \approx 5 \times 10^{-4}$.

each domain, followed by the rest of the states which are populated in this regime of the $V_{SD}-E_z$ plane. This picture is markedly different from the assumption made previously (section III) where only two domains, blue and pink, exist (see Figure 4 bottom). Furthermore, in equilibrium at zero temperature, the line $E_z = E_z^*$ is the boundary line in the $V_{SD}-E_z$ plane, separating these populations, while in nonequilibrium the boundaries of the different domains are the transition channels discussed in section III.

The transition channels form the boundary domains because they designate the threshold conditions for insertion of an electron or a hole into the junction. Such an injected charge carrier brings with it excess energy of $\mu + (eV_{SD})/2$ which can be used to populate higher-energy states.

It is important to note that to change the population distribution among the two neutral molecular states (i.e., (02), (11)) a concurrent population change in states of different charge is needed. For example, let us revert to Figure 4 (top) and consider the transfer of population from (02) to (11) at E_z = 0.58 V/Å. The energy for this process is $\Delta E(02 \rightarrow 11) = 0.2$ eV. Naïvely, one would expect that a source−drain bias of V_{SD} = 0.4 V will be the threshold voltage for population of (11). In reality, however, the threshold is determined by a totally different process, namely, the injection of an electron from the leads, (02 → 12), which occurs only at ≈1.9 V. The reason for this odd-looking dependence is simply that at 10 K one must rely on injected charge carriers to transfer the available energy in the leads into the junction.

B. Steady-State Current. The nonzero steady-state current shown in the middle panel of Figure 6 appears in several distinct domains bounded by the transition channels of the junction:

(a) The purple domains designate regimes of zero current.

(b) The red triangle defined by the transition channels (02 → 12) and (11 → 01) indicates a high current regime which has strong contributions from both electron and hole currents due to the relatively high population of (02) and (11) seen in the left panel.

(c) The green colored area on the right is bounded by the four transition channels (02 → 01), (11 → 01), (02 → 12), and (11 → 12). Dominant contribution to the current comes from the (02 → 12) electronic transition, and it is weak due to the low population of the (02) state. In this regime, the hole conducting channel (11 → 01) is not active.

(d) The yellow triangular region located at the upper left corner is bounded by the transition channels (02 → 01) and (02 → 12). The current is solely due to holes passing through the (11 → 01) conducting channel. The current is intense due to the relatively high population of state (11). Interestingly, the current is not due to any of the transitions defining the domain boundaries. These transitions do not contribute, because either they are energetically inaccessible ((02 → 12)) or they change n_2 ((02 → 01)), a process that is weak because QD2 is not directly coupled to the leads.

C. Redfield Conductance Channels. The current domains depicted above give rise to sharp differential conductance peaks called "conductance channels" which are displayed in Figure 6 (right). These peaks reveal a richer picture than predicted by the DFT−Landauer theory of Figure 5. To be specific, the DFT−Landauer conductance channels coincide only partially with those of Redfield; for example at $E_z < E_z^*$, the (02 → 12) appears in both descriptions, but (11 → 01) does not appear in the DFT picture because 11 is the ground state of the DFT Hamiltonian only when $E_z > E_z^*$. Here the situation changes, and this channel becomes active when the gate field crosses E_i, where "i" is the intersection of the two channels. The reason for its activation in a much lower gate field is connected directly to the involvement of a nonequilibrium mixed state which is displayed as a light gray triangle in the left panel of Figure 6. To activate this channel one should have a significant population of the (11) state. In the KS/GKS picture, state (11) is not populated at all because $E_z < E_z^*$ (blue domain in Figure 4 (bottom)), but in the nonequilibrium mixture it carries a significant population and therefore is able to conduct.

A surprising finding was the appearance of additional conductance channels, absent from the DFT−Landauer picture. These channels appear as horizontal lines in Figure 6 (right) at V_{SD} = 1.4 V and V_{SD} = 2.2 V. These are attributed to the transition channels (11 → 12) and (02 → 01), respectively. Since these transition channels are not conducting (because they involve a change in the population of QD2, which is not directly coupled to the leads), their presence is somewhat surprising. This is a second example where the nonequilibrium

dx.doi.org/10.1021/jp312776c | J. Phys. Chem. C 2013, 117, 10257−10263

mixed states are important. At low gate field, the appearance of a mixed state at $V_{SD} > 2.2$ V which populates state (11) (see yellow triangle at the left panel of Figure 6) enables a hole conductance at gate fields much lower than E_z^*. At the same time the appearance of a mixed state at higher gate field which populates state (02) (see green pentagon at the left panel of Figure 6) enables an electron conductance at $E_z > E_z^*$.

V. SUMMARY

We have studied the conductance of the molecular junction depicted in Figure 1, under an external gate field and source−drain bias. This junction was considered in our previous paper where we studied the conductance using a ground-state Hamiltonian, based on a DFT for which the orbital energies are close to the quasiparticle energies and employing Landauer's formula[1] which describes the conductance of noninteracting particles. We showed that this Landauer + DFT approach is fundamentally flawed (needs an additional orbital) to account for all the nonequilibrium effects in this system. Using the data and insights provided by the DFT calculations, we built a double quantum-dot Hubbard Hamiltonian to describe this junction. We then employed a nonequilibrium many-body approach based on the Redfield theory to calculate the steady-state populations, current, and conductance channels of this junction. We used the same model Hamiltonian to construct the conductance channels of this junction at equilibrium population of molecular states, assuming zero temperature and employing the diabatic limit. This picture mimics the conductance calculated in ref 1 using the DFT−Landauer approach.

Whenever the Redfield approach produces a SSDM which strongly mixes the two ground states (02) and (11) our Landauer + DFT approach will fail since it always produces a Hamiltonian based on just one of the two states. We expected that the SSDM will mix these states only when the gate field E_z is close to the critical gate field E_z^* because then they are nearly degenerate. However, we found that the mixture is strong even when $E_z \ll E_z^*$, and thus the conductance map is more involved than anticipated.

One of the attractive features of the junction is the small number of conductance channels and the sharp response to the gate field. This was predicted in ref 1 based on the simplified but wrong Landauer + DFT approach. Within the more realistic Redfield approach additional conductance channels form, making the picture somewhat more intricate. However, the number of such channels is still very small, and the high tunability properties and sharp switching behavior of this junction (Figure 6 (right)) are preserved.

AUTHOR INFORMATION

Corresponding Author

*E-mail: roi.baer@huji.ac.il. Phone: +97226586108 (R.B.). E-mail: migalperin@ucsd.edu. Phone: +1-858-246-0511 (M.G.).

Notes

The authors declare no competing financial interest.

ACKNOWLEDGMENTS

RB gratefully thanks the Israel Science Foundation (ISF grant no. 1020-10) and the US-Israel Binational Science Foundation (BSF grant no. 2008221) for support of this work. MG gratefully thanks the Department of Energy (Early Career Award, DE-SC0006422) and the US-Israel Binational Science Foundation (grant no 2008282) for support of this research.

REFERENCES

(1) Baratz, A.; Baer, R. Nonmechanical Conductance Switching in a Molecular Tunnel Junction. *J. Phys. Chem. Lett.* **2012**, *3*, 498−502.
(2) Evers, F.; Weigend, F.; Koentopp, M. Conductance of Molecular Wires and Transport Calculations Based on Density-Functional Theory. *Phys. Rev. B* **2004**, *69*, 235411.
(3) Di Ventra, M.; Pantelides, S. T.; Lang, N. D. First-Principles Calculation of Transport Properties of a Molecular Device. *Phys. Rev. Lett.* **2000**, *84*, 979.
(4) Taylor, J.; Guo, H.; Wang, J. Ab Initio Modeling of Quantum Transport Properties of Molecular Electronic Devices. *Phys. Rev. B* **2001**, *63*, 245407.
(5) Brandbyge, M.; Mozos, J.-L.; Ordejón, P.; Taylor, J.; Stokbro, K. Density-Functional Method for Nonequilibrium Electron Transport. *Phys. Rev. B* **2002**, *65*, 165401.
(6) Landauer, R. Spatial Variation of Currents and Fields Due to Localized Scatterers in Metallic Conduction. *IBM J. Res. Dev.* **1957**, *1*, 223.
(7) Koentopp, M.; Chang, C.; Burke, K.; Car, R. Density Functional Calculations of Nanoscale Conductance. *J. Phys.: Condens. Matter* **2008**, *20*, 083203.
(8) Schmitteckert, P.; Evers, F. Exact Ground State Density-Functional Theory for Impurity Models Coupled to External Reservoirs and Transport Calculations. *Phys. Rev. Lett.* **2008**, *100*, 086401.
(9) Baer, R.; Livshits, E.; Salzner, U. "Tuned" Range-Separated Hybrids in Density Functional Theory. *Annu. Rev. Phys. Chem.* **2010**, *61*, 85−109.
(10) Stein, T.; Kronik, L.; Baer, R. Reliable Prediction of Charge Transfer Excitations in Molecular Complexes Using Time-Dependent Density Functional Theory. *J. Am. Chem. Soc.* **2009**, *131*, 2818−2820.
(11) Stein, T.; Eisenberg, H.; Kronik, L.; Baer, R. Fundamental Gaps of Finite Systems from the Eigenvalues of a Generalized Kohn-Sham Method. *Phys. Rev. Lett.* **2010**, *105*, 266802.
(12) Palacios, J. J. Coulomb Blockade in Electron Transport through a C_{60} Molecule from First Principles. *Phys. Rev. B* **2005**, *72*, 125424.
(13) Schoeller, H.; Schon, G. Mesoscopic Quantum Transport - Resonant-Tunneling in the Presence of a Strong Coulomb Interaction. *Phys. Rev. B* **1994**, *50*, 18436−18452.
(14) Utsumi, Y.; Martinek, J.; Schon, G.; Imamura, H.; Maekawa, S. Nonequilibrium Kondo Effect in a Quantum Dot Coupled to Ferromagnetic Leads. *Phys. Rev. B* **2005**, *71*, 245116.
(15) Leijnse, M.; Wegewijs, M. R. Kinetic Equations for Transport through Single-Molecule Transistors. *Phys. Rev. B* **2008**, *78*, 235424.
(16) Koller, S.; Grifoni, M.; Leijnse, M.; Wegewijs, M. R. Density-Operator Approaches to Transport through Interacting Quantum Dots: Simplifications in Fourth-Order Perturbation Theory. *Phys. Rev. B* **2010**, 82.
(17) Ovchinnikov, I. V.; Neuhauser, D. A Liouville Equation for Systems Which Exchange Particles with Reservoirs: Transport through a Nanodevice. *J. Chem. Phys.* **2005**, *122*, 024707.
(18) Schaller, G.; Kiesslich, G.; Brandes, T. Transport Statistics of Interacting Double Dot Systems: Coherent and Non-Markovian Effects. *Phys. Rev. B* **2009**, *80*, 245107.
(19) Pedersen, J. N.; Wacker, A. Tunneling through Nanosystems: Combining Broadening with Many-Particle States. *Phys. Rev. B* **2005**, *72*, 195330.
(20) Esposito, M.; Galperin, M. Transport in Molecular States Language: Generalized Quantum Master Equation Approach. *Phys. Rev. B* **2009**, *79*, 205303.
(21) Esposito, M.; Galperin, M. Self-Consistent Quantum Master Equation Approach to Molecular Transport. *J. Phys. Chem. C* **2010**, *114*, 20362−20369.

(22) Wingreen, N. S.; Meir, Y. Anderson Model out of Equilibrium - Noncrossing-Approximation Approach to Transport through a Quantum-Dot. *Phys. Rev. B* **1994**, *49*, 11040−11052.
(23) Sivan, N.; Wingreen, N. S. Single-Impurity Anderson Model out of Equilibrium. *Phys. Rev. B* **1996**, *54*, 11622−11629.
(24) Hettler, M. H.; Kroha, J.; Hershfield, S. Nonequilibrium Dynamics of the Anderson Impurity Model. *Phys. Rev. B* **1998**, *58*, 5649−5664.
(25) Eckstein, M.; Werner, P. Nonequilibrium Dynamical Mean-Field Calculations Based on the Noncrossing Approximation and Its Generalizations. *Phys. Rev. B* **2010**, *82*, 115115.
(26) Oh, J. H.; Ahn, D.; Bubanja, V. Transport Theory of Coupled Quantum Dots Based on the Auxiliary-Operator Method. *Phys. Rev. B* **2011**, *83*, 205302.
(27) White, A. J.; Galperin, M. Inelastic Transport: A Pseudoparticle Approach. *Phys. Chem. Chem. Phys.* **2012**, *14*, 13809−13819.
(28) White, A. J.; Fainberg, B. D.; Galperin, M. Collective Plasmon-Molecule Excitations in Nanojunctions: Quantum Consideration. *J. Phys. Chem. Lett.* **2012**, *3*, 2738−2743.
(29) Sandalov, I.; Johansson, B.; Eriksson, O. Theory of Strongly Correlated Electron Systems: Hubbard-Anderson Models from an Exact Hamiltonian, and Perturbation Theory near the Atomic Limit within a Nonorthogonal Basis Set. *Int. J. Quantum Chem.* **2003**, *94*, 113−143.
(30) Fransson, J. Nonequilibrium Theory for a Quantum Dot with Arbitrary on-Site Correlation Strength Coupled to Leads. *Phys. Rev. B* **2005**, *72*.
(31) Sandalov, I.; Nazmitdinov, R. G. Shell Effects in Nonlinear Magnetotransport through Small Quantum Dots. *Phys. Rev. B* **2007**, *75*, 075315.
(32) Galperin, M.; Nitzan, A.; Ratner, M. A. Inelastic Transport in the Coulomb Blockade Regime within a Nonequilibrium Atomic Limit. *Phys. Rev. B* **2008**, *78*, 125320.
(33) Yeganeh, S.; Ratner, M. A.; Galperin, M.; Nitzan, A. Transport in State Space: Voltage-Dependent Conductance Calculations of Benzene-1,4-dithiol. *Nano Lett.* **2009**, *9*, 1770−1774.
(34) Lindblad, G. Generators of Quantum Dynamical Semigroups. *Commun. Math. Phys.* **1976**, *48*, 119−130.
(35) Davies, E. B. *Quantum Theory of Open Systems*; Academic Press: London; New York, 1976.
(36) Kohen, D.; Marston, C. C.; Tannor, D. J. Phase Space Approach to Theories of Quantum Dissipation. *J. Chem. Phys.* **1997**, *107*, 5236−5253.
(37) Breuer, H.-P.; Petruccione, F. *The Theory of Open Quantum Systems*; Oxford University Press: Oxford; New York, 2002.
(38) Nitzan, A. *Chemical Dynamics in Condensed Phases: Relaxation, Transfer and Reactions in Condensed Molecular Systems*; Oxford University Press: Oxford; New York, 2006.
(39) Harbola, U.; Esposito, M.; Mukamel, S. Quantum Master Equation for Electron Transport through Quantum Dots and Single Molecules. *Phys. Rev. B* **2006**, *74*, 235309.
(40) The total gate bias is a sum of the gate potential V_0 and the gate bias V_G, both adjustable (see Figure 1); the source−drain bias V_{SD} is also adjustable. Therefore our scheme describes the situation where the total gate field and source−drain bias are changing while keeping $(\mu\text{-}V_0)$ fixed.
(41) The term conducting channel is a conductance peak as a function of the source−drain potential difference and gate field.